



OPEN A single-center prospective study evaluating the relationship of tumor consistency on remission in acromegaly patients

Eren Yilmaz¹, Seda Duman Ozturk², Ayse Uzuner³, Pinar Yildirim³, Atakan Emengen⁴, Aykut Gokbel⁴, Melih Caklili³, Sibel Balci⁵, Ayca Ersen Danyeli⁶, Burak Cabuk³, Ihsan Anik³ & Savas Ceylan⁴✉

The nature of somatotroph adenomas has not been clearly revealed in studies. We consider that there are macroscopic differences in intraoperative tumor consistency in acromegaly patients. We aimed to determine whether there is a relationship between intraoperative tumor consistency and histopathological subtypes by planning a prospective study to determine whether these differences are significant. Between August 1997 and December 2021, 1118 patients with GH-secreting tumors underwent endoscopic endonasal surgery at our Pituitary Research Center. Between January 2022 and May 2023, pure GH-secreting adenomas operated via the endoscopic endonasal approach were sequentially categorized into three types (Type-1: Soft, Type-2: Mucinous/Adhesive, Type-3: Mix/Intermediate) according to the intraoperative tumor consistency. The final patient cohort consisted 218 cases. The ratio of densely granulated adenomas (DG-A) to sparsely granulated adenomas (SG-A) was as follows: Type-1, 89/11; Type-2, 5/95; Type-3, 13/5. Logistic regression revealed that Type-1 tumors were associated with a high remission rate ($p = 0.011$), and Type-2 were associated with SG-A ($p < 0.001$). Furthermore, no or weak staining for E-cadherin was associated with Type-2 tumors ($p < 0.001$). Surgeon could predict the prognosis and histopathological subtype of the pure somatotroph adenoma by observing the intraoperative tumor consistency. This could facilitate better intraoperative planning of patient-specific surgical strategies to increase the remission rates.

Keywords Acromegaly, Tumor consistency, Histopathological subtypes

Abbreviations

CSI	Cavernous sinus invasion
DG-A	Densely granulated somatotroph adenoma
GH	Growth hormone
GTR	Gross total resection
H&E	Hematoxylin and eosin
IGF-I	Insulin like growth factor-1
MRI	Magnetic resonance imaging
OGTT	Oral glucose tolerance test
SG-A	Sparsely granulated somatotroph adenoma
STR	Subtotal resection

Approximately 10–15% of pituitary adenomas produce growth hormone (GH)^{1,2}. According to the 2022 WHO Classification of Pituitary Tumors, there are various tumor types in the pituitary gland that secrete GH³, including pure somatotroph tumors (sparsely/densely granulated), plurihormonal tumors (mammotroph, mixed, and mature plurihormonal PIT-1 lineage tumors), and, rarely, acidophil stem cell tumors and immature PIT-1

¹Department of Neurosurgery, Cihanbeyli State Hospital, Konya, Turkey. ²Department of Pathology, Kocaeli University School of Medicine, Kocaeli, Turkey. ³Department of Neurosurgery, Pituitary Research Center, Kocaeli University School of Medicine, Kocaeli, Turkey. ⁴Department of Neurosurgery, Bahcesehir University School of Medicine, Istanbul, Turkey. ⁵Department of Biostatistics and Medical Informatics, Kocaeli University, Kocaeli, Turkey. ⁶Department of Pathology, Acibadem University, Istanbul, Turkey. ✉email: ssceylan@yahoo.com

lineage tumors. These tumors express transcription factors and biomarkers and belong to the PIT-1 gene family. Ectopic GH production is rare⁴. Furthermore, pure somatotroph tumors are the most commonly observed tumor in patients with acromegaly.

The subtypes of pure somatotroph adenomas were defined in 1983 by Melmed et al. on the basis of their ultrastructural features under electron microscopy⁵. These subtypes are sparsely granulated somatotroph adenoma (SG-A) and densely granulated somatotroph adenoma (DG-A). Studies conducted using cytokeratin immunohistochemistry have demonstrated that these subtypes exhibit different nuclear staining patterns⁶. SG-As consist of cells demonstrating a dot distribution pattern on histopathology, while DG-As consist of cells exhibiting a perinuclear distribution pattern^{6,7}. Some authors have reported the existence of another subtype of somatotroph adenomas that are referred to as 'borderline' or 'transitional zone'. These are often classified within the DG-A type because they clinically and histopathologically resemble DG-As^{3,8,9}. The clinical features, prognosis, radiological appearances, response to adjuvant therapy, and other parameters of these subtypes have been the subject of numerous studies to date^{9–13}.

Currently, the remission rates of somatotroph adenomas range between 33 and 84%, which are still unsatisfactory^{9,12,14–19}. Studies to identify novel surgical, medical and radiosurgery treatments to increase remission rates are ongoing. Based on our experience with endoscopic endonasal pituitary surgery performed on 1118 acromegaly patients in our center between August 1997 and December 2021, we noticed macroscopic differences in intraoperative tumor consistency in acromegaly patients. Although there are studies regarding tumor consistency in pituitary adenomas^{20–22}, no study has specifically evaluated the relationship between tumor consistency and histopathological subtypes in pure somatotroph adenomas. Thus, in our study we aimed to identify the existence of a relationship between intraoperative tumor consistency and the histopathological tumor subtype in pure somatotroph adenomas. Furthermore, we aimed to determine whether the macroscopic differences observed intraoperatively could aid in the prediction of the adenoma's histopathological subtype, and if this prediction could aid in determining surgical strategy and increasing remission rates.

Methods

Patients

We planned a prospective study to investigate both the immunohistochemical results and the histopathological basis of different tumor consistencies noticed during the intraoperative period in acromegaly patients, as well as to evaluate surgical outcomes. Informed consent was obtained from patients participating in the study and/or their legal guardians. Approval for the study was received by the Kocaeli University Clinical Research Ethics Committee (project number: GOKAEK/294) and the study was carried out in accordance with international guidelines/regulations. The study began in January 2022. Pure GH-secreting adenomas, which were operated consecutively via the endoscopic endonasal approach, were divided into two categories (Type-1 and Type-2) according to their intraoperative consistency. Type-1 (Fig. 1) consisted of tumors that appeared white macroscopically, were freely suckable, and were easily resectable with surgical manipulation (Video 1/Case-1). Type-2 (Fig. 2) consisted of tumors that appeared muted-gray macroscopically, adhered to the surrounding tissues, were mucinous consistency in itself, were partially absorbable, and required radical manipulations for resection (Video 1/Case-2). The sample size of each group was determined as 100. The study also included a third group, "Type-3", which included 18 tumors that could not be definitively included intraoperatively in the other groups. Type-3 (Fig. 3) tumors consisted of tumors that macroscopically showed characteristics of both Type-1 and Type-2 tumors (Video 1/Case-3). When the Type-1 and Type-2 groups reached 100 cases each (in May 2023), the case categorization process was stopped. Approximately 3 months after the Type-1 group reached 100 cases, the Type-2 group reached 100 cases. Finally, the study cohort consisted of 218 cases. Patients with a history of previous surgery, cystic adenomas, co-secreting tumors (plurihormonal), and preoperative medical/radiosurgery treatment were not included in the study. The demographic and clinical data of the study patients were recorded, and the patients were followed up until May 2024.

Endocrine analysis

The preoperative GH and IGF-I levels and anterior pituitary functions of all the patients were tested in the same laboratory. If necessary, hormone replacement therapy was administered preoperatively to patients who demonstrated clinical and laboratory hypopituitarism. Following basal GH and IGF-I level measurements, all patients underwent an oral glucose tolerance test (OGTT) that was administered by endocrinologists and were diagnosed with acromegaly. Postoperative remission were evaluated using the 2019 consensus guideline²³ and categorized as early and late remission. A fasting GH level of < 1.0 µg/L on the 1st or 2nd postoperative day was considered as "early remission". Patient was considered to be in late remission if a random GH level measured in the 3rd postoperative month was < 1.0 µg/L, the post-OGTT GH level was < 0.4 µg/L, and the IGF-I level was < 1.2 times the upper limit according to age/sex²³. The patients were followed up every 3 months for the first year and every 6 months thereafter. Adjuvant treatments (medical/radiosurgery) were administered to patients who did not meet the remission criteria in the 3rd postoperative month. These patients were included in a controlled remission group.

Image analysis

Magnetic resonance imaging (MRI) was performed using a 3T MRI system (Achieve Intera Release, Philips, Eindhoven, The Netherlands). The preoperative and postoperative (1st day, 3rd month, 6th month, 12th month) T1- and T2-weighted MR images with and without contrast were evaluated in the sagittal and coronal planes. The radiological images were evaluated by a neuroradiologist and neurosurgeon under the following parameters: T2 signal intensity, presence/absence of cavernous sinus invasion (CSI), adenoma size, and amount of resection. According to the adenoma size, the tumor was classified as follows: microadenoma, if the maximum dimension

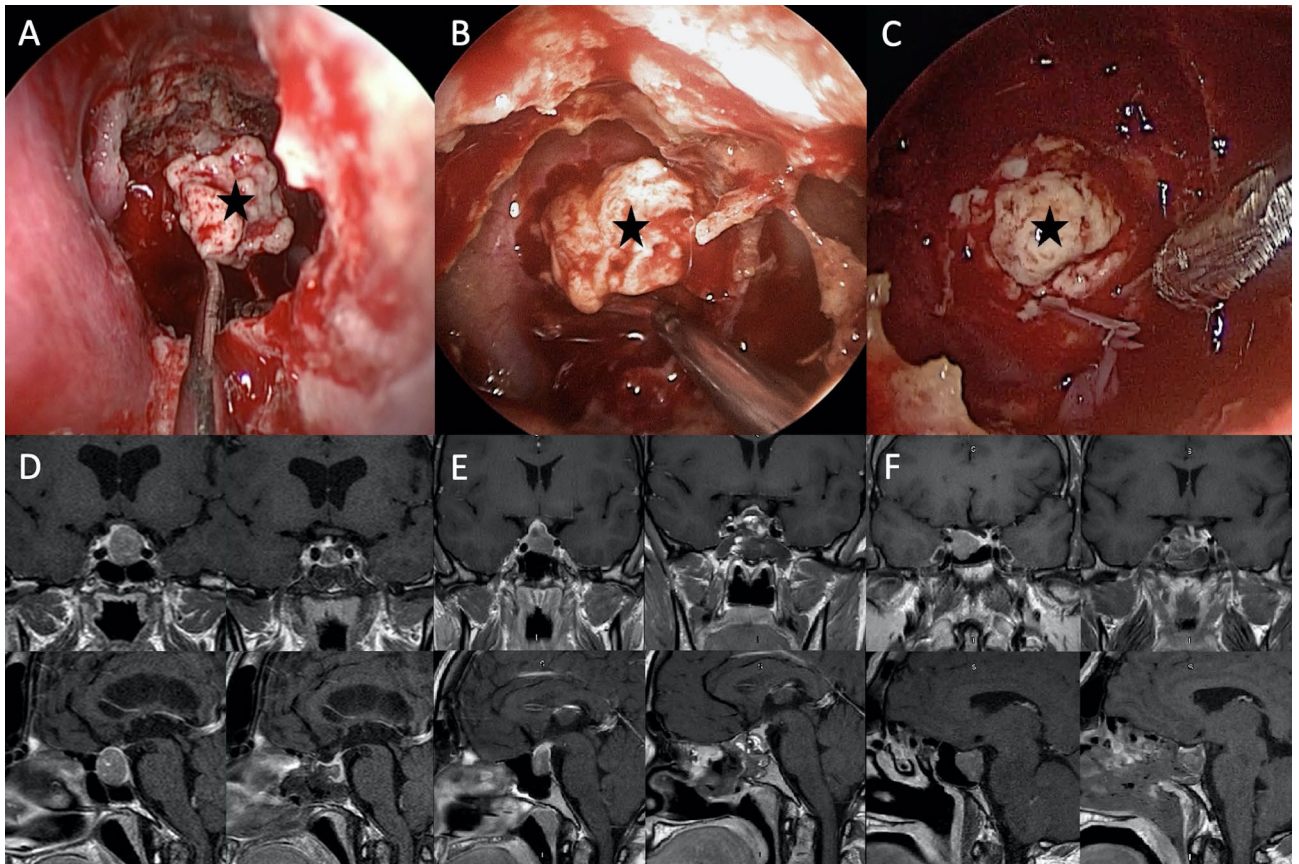


Fig. 1. (A–C): 3 different patients with Type-1 tumor consistency. Black star: Appearance of a white, non-fluid and non-mucinous, easily resectable adenoma. (D–F) Preoperative and postoperative MRI view.

on a single axis was < 1 cm; macroadenoma, if the tumor was 1–4 cm in size; and giant adenoma, if ≥ 4 cm in size. No residual tumor on contrast-enhanced T1-weighted sellar MRI obtained within the first 24 h after the surgery was considered as gross total resection (GTR), and some residual tumor was considered as subtotal resection (STR). In the preoperative period, the adenomas were classified according to their intensity in comparison with that of the gray and white matter of the temporal lobe on T2-weighted MR images^{24,25}. The adenomas were classified as follows: hypointense, when the signal intensity was equal to or lower than that of the white matter; hyperintense, when the signal intensity was equal to or higher than that of the gray matter; and isointense, when the signal intensity ranged between that of the white and gray matter.

Pathological evaluation

All tumors were evaluated by a pathologist blinded to the patient groups. Paraffin-embedded blocks were created from resected tissues that were fixed with 10% buffered formalin. The paraffin-embedded blocks were sectioned and stained with hematoxylin and eosin (H&E) and reticulin stains to confirm the presence of adenomas. Simultaneously, additional tumor tissues were used to create different specimen blocks using the tissue microarray method.

Cam5.2(mouse monoclonal antibody), gh(rabbit polyclonal antibody), prolactin, pit-1(ZM385 mouse monoclonal antibody), E-cadherin(mouse monoclonal antibody), and β -catenin(mouse monoclonal antibody) immunohistochemistry staining was performed using a fully automatic machine (Ventana Medical Systems [SN: 714592, Ref: 750–700], Arizona, USA). The sections were evaluated using positive and negative controls. Cam5.2 staining was used for the pathological subtype classification of the tumors.

Cam5.2 staining was evaluated according to the criteria used by Obari et al. as follows: perinuclear or ring-like pattern (none, < 70%, or $\geq 70\%$), fibrous bodies (none, 1–8%, 9–69%, or $\geq 70\%$) and migration pattern (none, < 70%, or $\geq 70\%$)⁸. Any cytoplasmic staining pattern that was not ring-like or fibrous was considered a transitional pattern.

The tumor subtypes were categorized as follows: DG-A, perinuclear pattern $\geq 70\%$ or fibrous bodies $\leq 8\%$; SG-A, punctate pattern $\geq 70\%$; intermediate form, perinuclear pattern < 70% and fibrous pattern $> 8\%$ ⁸. Subsequently, adenomas classified as ‘intermediate’ were included in the DG-A category due to their close clinical, biochemical, radiological and prognostic similarities to DG-As^{3,8,9,26}.

Immunostaining with gh, β -catenin, and E-cadherin was assessed in a semi-quantitative manner using the immunoreactivity scoring system^{9,11}. Immunoreactivity score (IRS) was determined by first calculating the percentage of positive tumor cells staining (0, none; 1, < 10%; 2, 10–50%; 3, 51–80%; and 4, > 80%). Based on

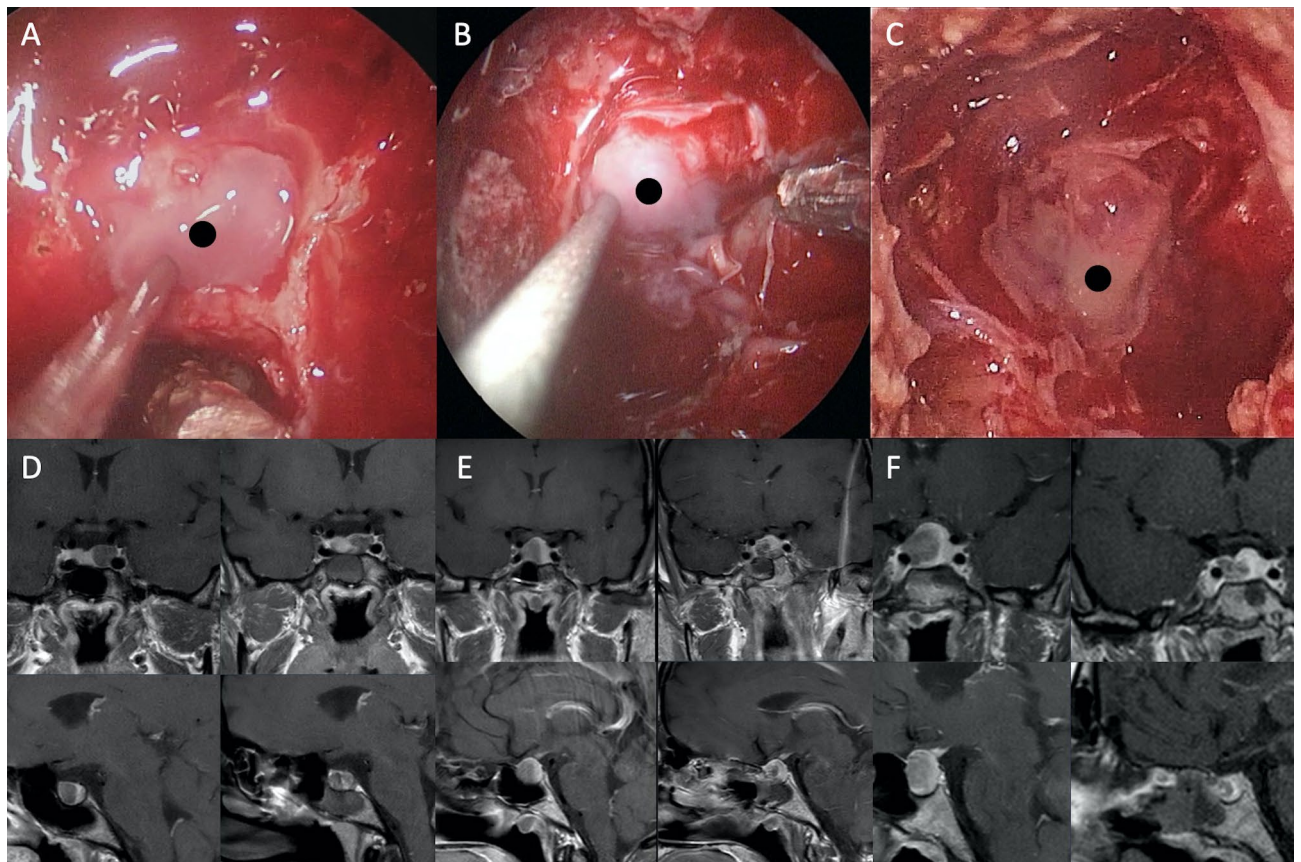


Fig. 2. (A–C) 3 different patients with Type-2 tumor consistency. Black circle: View of the adenoma with muted-gray color and fluidic-mucinous consistency. (D–F) Preoperative and postoperative MRI view.

the staining intensity (0, absent; 1, weak; 2, moderate; 3, strong), a score from 0 to 12 was obtained (0–3, low score; 4–6, medium score; 7–12, high score).

Statistical analysis

All statistical analyses were performed using SPSS for Windows (version 29.0; IBM Corp., Armonk, NY, USA). The Kolmogorov–Smirnov and Shapiro–Wilk tests were used to assess the normality of the data. The continuous variables are presented as medians and interquartile ranges (IQR) because the normality assumption did not hold. The categorical variables are presented as counts and percentages. Comparisons between the groups were carried out using the Kruskal–Wallis test. Dunn’s test was used for multiple comparisons. Associations between the categorical variables were examined using the Chi-square test. Multivariable analysis was performed using the logistic regression analysis. A *p*-value of < 0.05 was considered statistically significant.

Results

Patient characteristics

The female/male ratio was 122/96. The median age of the patients was 40 years (IQR: 33–50 years). The follow-up period was $19.88 \pm 4.97^{12-28}$ months. Demographic data of the patients, tumor size, CSI, MR-T2 intensities, and pre-operative GH levels are detailed in Table 1. The Type-1 group had significantly more microadenomas than the Type-2 group, and the Type-2 group had significantly more macroadenomas or giant adenomas than the Type-1 group ($p = 0.04$). The difference in the presence of CSI was not significant between the groups ($p = 0.095$). There were significantly more hyperintense adenomas on MR-T2 imaging in the Type-2 group compared to the Type-1 and Type-3 groups ($p < 0.001$). Furthermore, there were significantly more hypointense tumors on MR-T2 imaging in the Type-1 group compared to the Type-2 group ($p < 0.001$). The preoperative basal GH levels showed no correlation between the groups (Types-1, 2, and 3) ($p = 0.859$).

Endocrinological outcomes following treatment

Postoperative surgical and endocrinological outcomes of the patients are detailed in Table 1. GTR was achieved in 151 (69.3%) patients. Early postoperative remission was seen in 139 (63.8%) patients. The univariate analysis revealed that the Type-1 group had a significantly higher GTR ratio than the Type-2 group ($p = 0.011$). Patients in the Type-1 group had a higher probability of both early and late remission than patients in the Type-2 group ($p = 0.004$ and $p = 0.038$, respectively).

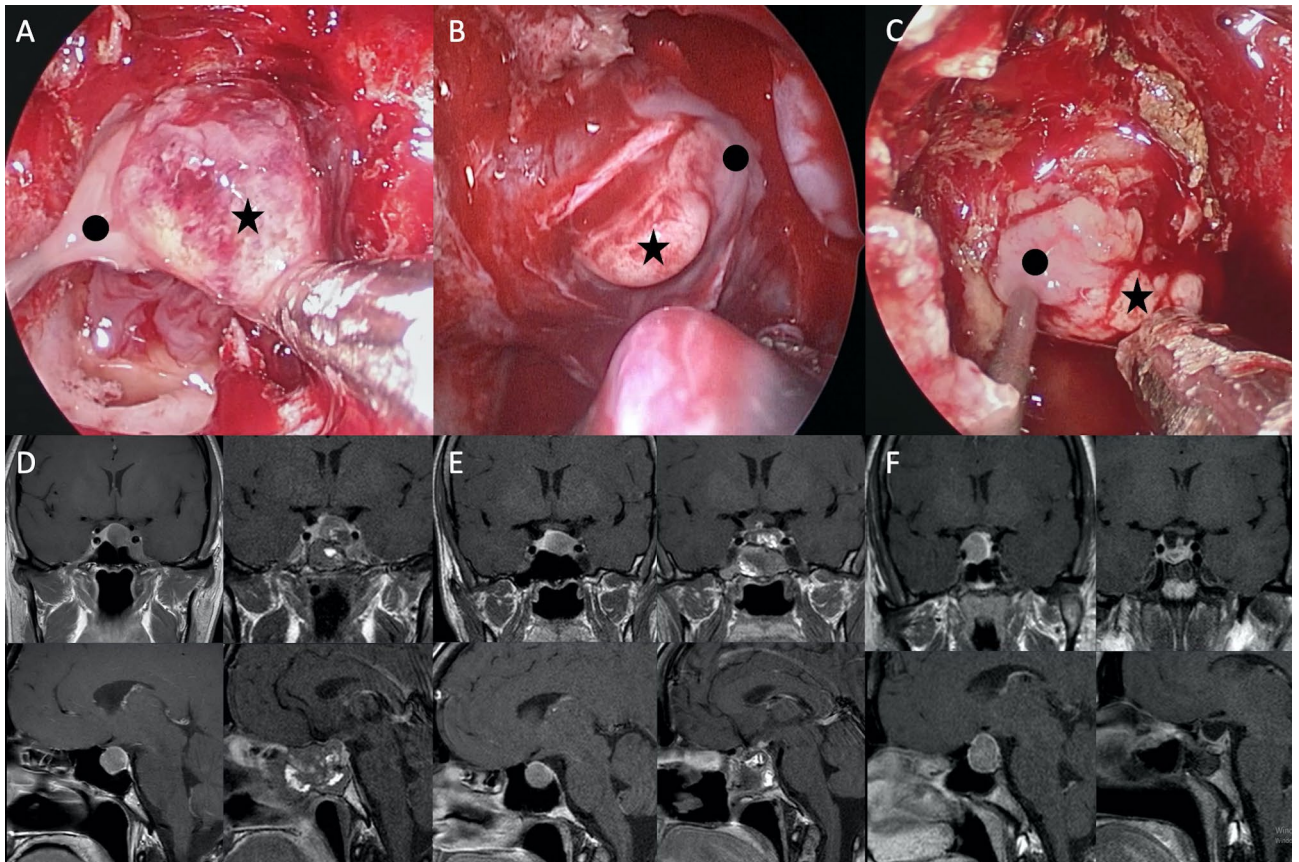


Fig. 3. (A–C) 3 different patient examples included in the Type-3 group. It contains both areas with Type-1 tumor consistency (black star) and areas with Type-2 tumor consistency (black circle). (D–F) Preoperative and postoperative MRI view.

Adjuvant treatment was administered to 77 of the 79 patients who did not meet the remission criteria at their 3rd postoperative examination (Type-1, $n=26$; Type-2, $n=45$; Type-3, $n=6$). Medical treatment alone was administered to 64 patients, radiosurgery and medical treatment to 12 patients, and radiosurgery alone to 1 patient). The remission rates of adjuvant therapy among the groups were as follows: Type-1, 80.8% ($n=21$); Type-2, 26.7% ($n=12$); and Type-3, 50% ($n=3$). Univariate analysis revealed that the remission rates following adjuvant treatment were significantly higher in the Type-1 group than in the Type-2 group ($p < 0.001$).

During the follow-up period, no patient underwent reoperation due to recurrence. However, six patients (2.7%) underwent surgery for rhinorrhea in the postoperative period. 20.6% of the patients ($n=45$) developed new endocrine insufficiency in at least one axis. Of these 45 patients, 22 (48.9%) were in the Type-1 group, 20 (44.4%) in the Type-2 group, and 3 (6.7%) in the Type-3 group. The rates of new postoperative endocrine insufficiency in at least one axis did not significantly differ between the groups ($p=0.850$).

Histopathological outcomes

According to the Cam5.2 immunohistochemistry staining pattern, 111 patients (50.9%) had DG-A and 107 (49.1%) had SG-A. Histopathological outcomes of the groups are shared in detail in Table 1. Univariate analysis revealed that the relationship between Type-1 tumor consistency and DG-A was significantly stronger than the relationship between Type-2 tumor consistency and DG-A ($p=0.001$) (Fig. 4/A, B,E). The relationship between Type-2 tumor consistency and SG-A was significantly stronger than the relationship between Type-1 or Type-3 tumor consistency and SG-A ($p=0.001$) (Fig. 5/A, B,E).

The IRS score following E-cadherin and β -catenin staining was low in 114 (52.3%) patients and was high in 104 (47.7%) patients. 92 of 104 cases were Type-1 (88.5%) (Fig. 4C/D), 97 of 114 cases were Type-2 (85.1%) (Fig. 5C/D). In the type-3 group, the IRS score following E-cadherin and β -catenin staining was low in 9(50%) cases and high in 9(50%) cases (Fig. 6). The loss of E-cadherin and β -catenin staining was significantly higher rate in the Type-2 group than in the Type-1 group ($p=0.001$).

Logistic regression analysis

Four different logistic regression models were constructed to determine the factors that could influence tumor consistency, resection, remission, and histopathological subtype (SG-A/DG-A) (Table 2). Parameters that were statistically significant in the univariate analyses were included in the multiple logistic regression model. However, β -catenin was not included in the models because it caused multicollinearity issues.

Variables	Total (n = 218)	Type-1 (n = 100)	Type-2 (n = 100)	Type-3 (n = 18)	p
Age (years), median (IQR)	40 (33–50)	44 (36–52) ^a	38 (31–45.75) ^b	37.5 (32.5–56.75) ^{ab}	0.003
Gender, n (%)					0.026
Female	122 (56)	46 (46) ^a	64 (64) ^b	12 (66.7) ^{ab}	
Male	96 (44)	54 (54) ^a	36 (36) ^b	6 (33.7) ^{ab}	
Tumor size, n (%)					0.049
Micro adenoma	36 (16.5)	23 (23) ^a	10 (10) ^b	3 (16.7) ^{ab}	
Macro/giant adenoma	182 (83.5)	77 (77) ^a	90 (90) ^b	15 (83.3) ^{ab}	
CS invasion, n (%)					0.095
Yes	31 (14.2)	10 (10)	16 (16)	5 (27.8)	
No	187 (85.8)	90 (90)	84 (84)	13 (72.2)	
MR-T2 image, n (%)					< 0.001
Hypo-intense	103 (47.2)	79 (79) ^a	14 (14) ^b	10 (55.5) ^a	
Iso-intense	24 (11.0)	7 (7) ^a	12 (12) ^{ab}	5 (27.8) ^b	
Hyper-intense	91 (41.7)	14 (14) ^a	74 (74) ^b	3 (16.7) ^a	
Preoperative GH level (µg/L), n (%)					0.859
0–20	159 (72.9)	73 (73)	74 (74)	12 (66.6)	
20–40	38 (17.4)	17 (17)	18 (18)	3 (16.6)	
> 40	21 (9.6)	10 (10)	8 (8)	3 (16.6)	
Histopathological subtype, n (%)					< 0.001
SG-A	111 (50.9)	11 (11) ^a	95 (95) ^b	5 (27.8) ^a	
DG-A	107 (49.1)	89 (89) ^a	5 (5) ^b	13 (72.2) ^a	
GH (IHC) staining, n (%)					< 0.001
Weak/moderate	104 (47.7)	3 (3) ^a	97 (97) ^b	4 (22.2) ^c	
Strong	114 (52.3)	97 (97) ^a	3 (3) ^b	14 (77.8) ^c	
E-kadherin staining, n (%)					< 0.001
No/weak	114 (52.3)	8 (8) ^a	97 (97) ^b	9 (50) ^c	
Strong	104 (47.7)	92 (92) ^a	3 (3) ^b	9 (50) ^c	
Beta katenin, n (%)					< 0.001
No/weak	114 (52.3)	8 (8) ^a	97 (97) ^b	9 (50) ^c	
Strong	104 (47.7)	92 (92) ^a	3 (3) ^b	9 (50) ^c	
Ki67 Index, n (%)					0.862
< 3	73 (33.5)	32 (32)	34 (34)	7 (38.9)	
≥ 3	145 (66.5)	68 (68)	66 (66)	11 (61.1)	
Resection, n (%)					0.015
GTR	151 (69.3)	79 (79) ^a	60 (60) ^b	12 (66.7) ^{ab}	
STR	67 (30.7)	21 (21) ^a	40 (40) ^b	6 (33.3) ^{ab}	
Early remission, n (%)					0.005
Yes	139 (63.8)	75 (75) ^a	53 (53) ^b	11 (61.1) ^{ab}	
No	79 (36.2)	25 (25) ^a	47 (47) ^b	7 (38.9) ^{ab}	
Delayed remission, n (%)					0.043
Yes	139 (63.8)	72 (72) ^a	55 (55) ^b	12 (66.7) ^{ab}	
No	79 (36.2)	28 (28) ^a	45 (45) ^b	6 (33.3) ^{ab}	
Controlled remission, n (%)					< 0.001
Yes	175 (80.3)	93 (93) ^a	67 (67) ^b	15 (83.3) ^{ab}	
No	43 (19.7)	7 (7) ^a	33 (33) ^b	3 (16.7) ^{ab}	

Table 1. Analysis of patient and tumor characteristics with tumor consistency. SG-A: Sparsely granulated adenoma, DG-A: Densely granulated adenoma, CS: Cavernous sinus, GTR: Gross total resection, STR: Subtotal resection, IQR: Interquartile range. Different uppercase letters indicate statistically significant differences between tumor consistency types.

Tumor consistency, tumor size, and CSI were included in the models constructed to predict the resection type and early remission. These models revealed that a Type-1 tumor, microadenoma, and absence of CSI were positive predictors of higher GTR ($p = 0.022$, $p = 0.035$, and $p < 0.001$, respectively) and early remission rates ($p = 0.011$, $p = 0.013$, and $p < 0.001$, respectively).

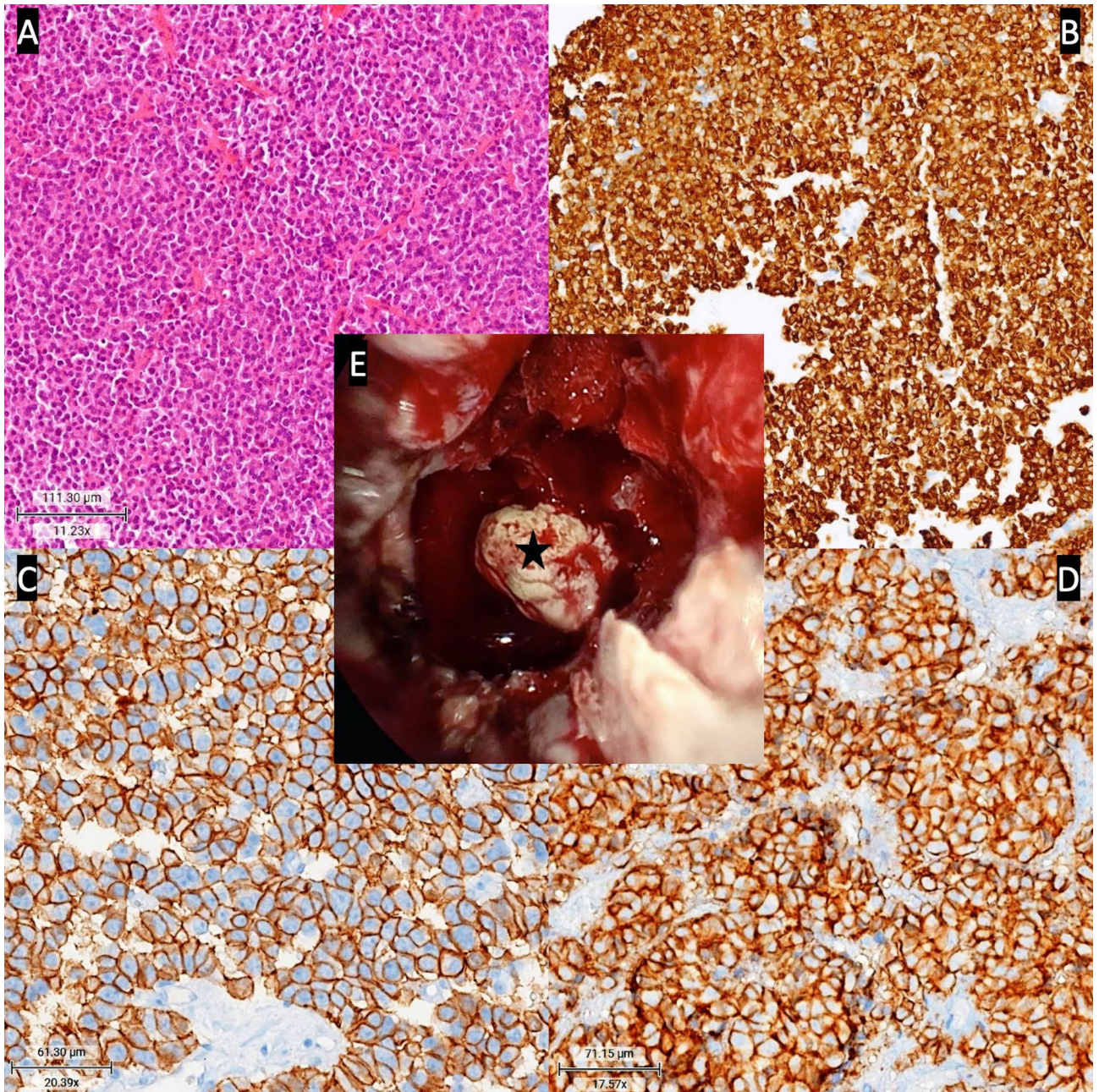


Fig. 4. (A) Microscopic view of densely granular somatotroph tumor, Hematoxylin and Eosin. (B) Diffuse cytoplasmic staining with Cam5.2 immunohistochemistry stain. (C) Diffuse membranous staining with E-Cadherin immunohistochemical stain. (D) Diffuse staining with beta catenin immunohistochemical stain. (E) Intraoperative view of adenoma (black star) with Type-1 tumor consistency.

Tumor consistency and tumor intensity on T2-sequences were included in the model to predict histopathological type (SG-A/DG-A). The model revealed that Type-2 tumors and hyperintense tumors were significant predictors of SG-A ($p < 0.001$ and $p < 0.001$, respectively).

E-cadherin staining and tumor intensity on T2- sequences were included in the model to predict tumor consistency. The model revealed that no or weak staining for E-cadherin and hyperintense adenomas were significant predictors of Type-2 tumors ($p < 0.001$ and $p = 0.001$, respectively).

Discussion

Somatotroph adenomas have classified according to the cytokeratin immunohistochemical staining patterns^{3,6,7} as SG-A and DG-A. However, there is a third subtype, which is defined as the 'intermediate form' or 'transition zone'. The clinical, prognostic, and surgical results and the histopathological features of the three subtypes have been examined by numerous authors⁹⁻¹³. However, no study has evaluated intraoperative tumor consistencies in

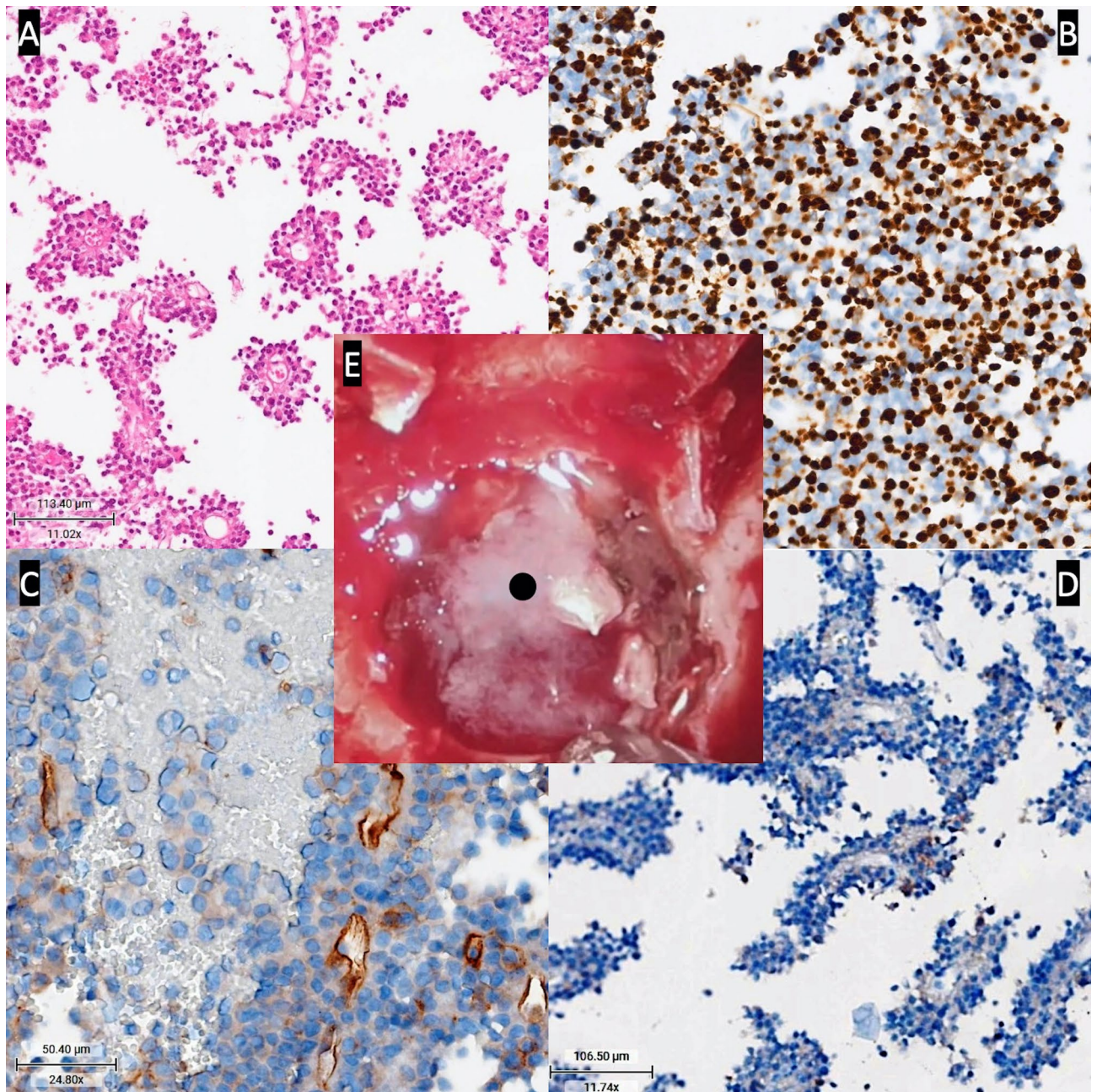


Fig. 5. (A) Microscopic view of sparsely granular somatotroph tumor, Hematoxylin and Eosin. (B) Diffuse fibrous body staining with Cam5.2 immunohistochemistry stain. (C) Diffuse loss of expression in E-Cadherin immunohistochemical stain. (D) Diffuse loss of expression in Beta catenin immunohistochemical stain. (E) Intraoperative view of adenoma (black circle) with Type-2 tumor consistency.

pure somatotroph adenomas and determined its role as a predictor of the definitive histopathological subtypes. In our prospective study, we found that the intraoperative tumor consistency was strongly correlated with the histopathological subtypes. Type-1 tumors were strongly related to a DG-A diagnosis, and Type-2 tumors were strongly related to a SG-A diagnosis. The advantage of revealing this similarity is that the surgeon will be able to predict the histopathological subtype of the adenoma by observing the tumor consistency during the operation. Furthermore, this will allow the surgeons to determine the appropriate surgical strategy intraoperatively to increase the remission rate. Especially, the surgeon can adopt a more aggressive strategy in the presence of a Type-2 tumor due to its significant correlation with a SG-A diagnosis, which is invasive and associated with a low remission rate.

Molecules involved in the cell cycle, such as E-cadherin, play a crucial role in the invasion and progression of pituitary tumors. Cadherins, a family of calcium-dependent cell–cell adhesion glycoproteins, control solid tissue morphogenesis, including cell type separation, cell growth, cell differentiation, and maintenance of specific tissue architecture^{27–29}. Cadherins must form complexes with cytoplasmic plaque proteins such as β - or γ -catenin to

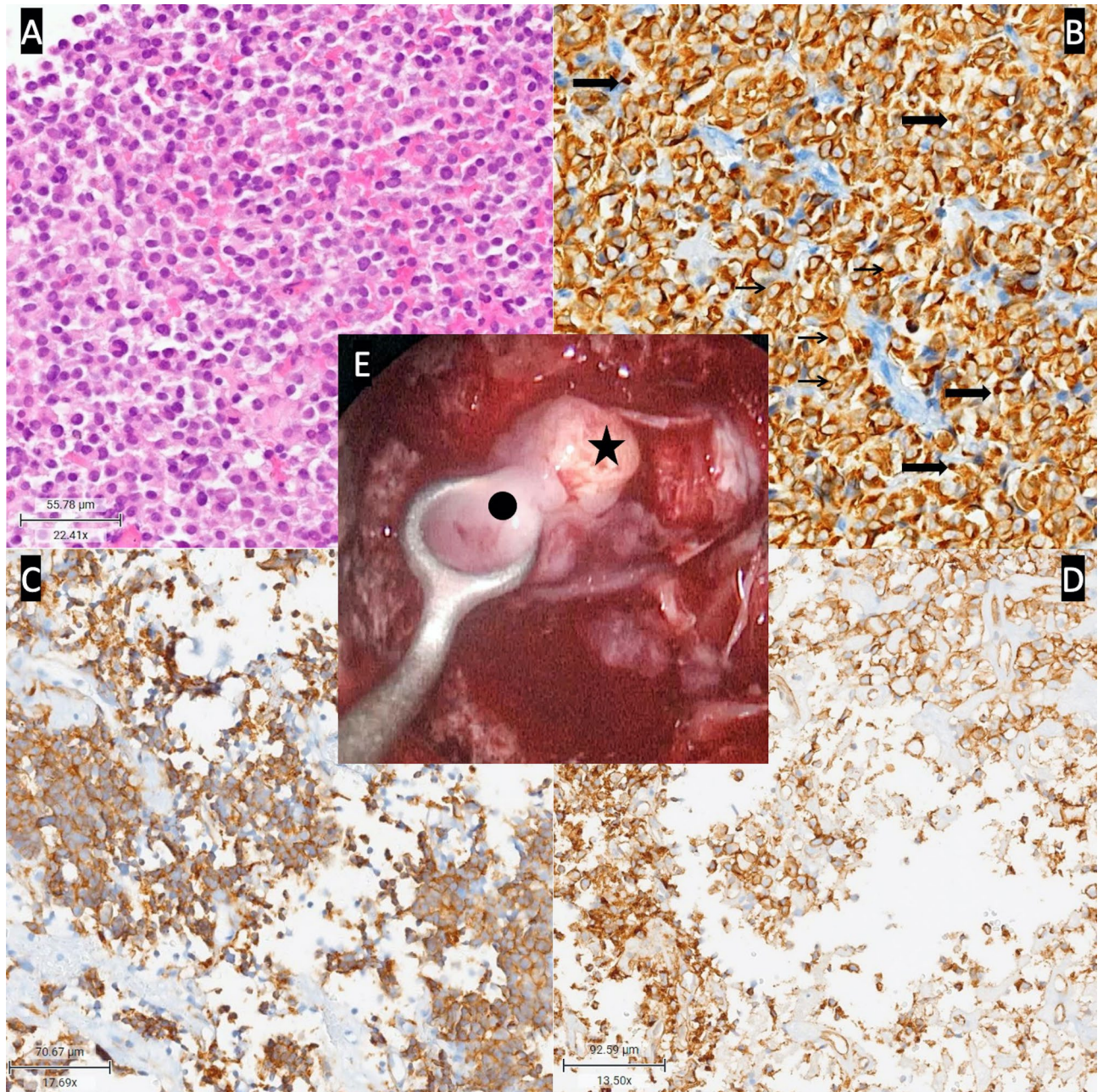


Fig. 6. (A) Microscopic view of intermediate form somatotroph tumor, Hematoxylin Eosin. (B) Diffuse cytoplasmic, partially fibrous body staining with Cam5.2 immunohistochemistry staining in intermediate form somatotroph tumors. (thick arrow shows fibrous body, thin arrow shows cytoplasmic staining). (C) Diffuse membranous staining with E-Cadherin immunohistochemical staining, focal loss of expression (D) Diffuse staining with beta catenin immunohistochemical stain, focal loss of expression. (E) Intraoperative view of adenoma in Type-3 tumor consistency. It contains both areas with Type-1 tumor consistency (black star) and areas with Type-2 tumor consistency (black circle).

exhibit functional adhesive activities²⁷. Loss of E-cadherin or its partners in cellular adhesion prevents neoplastic cells from adhering to each other, thus preventing the formation of solid tissue morphogenesis and increasing the invasive potential of neoplastic cells³⁰. Sano et al. demonstrated that somatotroph adenomas with intense fibrous bodies ($\geq 70\%$) lack adhesive properties and exhibit scattered tumor cells³¹. They noted that this occurs due to deficiencies or dysfunction in the cadherin and catenin families. Furthermore, intense fibrous bodies are a histopathological feature of SG-A^{3,8,9,26}. Therefore, the deficiency of cadherin and catenin in the SG-A subtype leads to the presence of tumor cells that do not show the ability to adhere to each other. The tumor tissue, formed by tumor cells that do not have the ability to adhere to each other, is expected to show a fluidic-mucinous form on a macroscopic scale, be invasive, and not have a solid tissue consistency. The immunohistochemistry results of our study revealed that 106 of the 111 patients with SG-A (95.5%) demonstrated no or weak staining for

Variable	OR (95% CI)	p	aOR (95% CI)	p
Early remission ^a				
Tumor consistency				
Type-1 (R)	1.0		1.0	
Type-2	0.37 (0.21–0.68)	0.001	0.43 (0.22–0.82)	0.011
Type-3	0.52 (0.18–1.49)	0.228	0.79 (0.23–2.67)	0.701
Tumor size				
Micro adenoma (R)	1.0		1.0	
Macro/giant adenoma	0.13 (0.04–0.43)	0.001	0.21 (0.06–0.71)	0.013
Cavernous sinus invasion				
Yes	0.09 (0.04–0.25)	<0.001	0.12 (0.05–0.32)	<0.001
No (R)	1.0		1.0	
Histopathological subtype ^b				
Tumor consistency				
Type-1 (R)	1.0		1.0	
Type-2	153.73 (51.38–459.96)	<0.001	76.42 (23.84–244.98)	<0.001
Type-3	3.11 (0.93–10.4)	0.065	3.06 (0.79–11.87)	0.106
T2-MRI				
Hypo-intense (R)	1.0		1.0	
Iso-intense	5.58 (2.16–14.44)	<0.001	1.94 (0.47–8.03)	0.361
Hyper-intense	34.34 (15.28–77.19)	<0.001	10.08 (3.37–30.16)	<0.001
Resection ^c				
Tumor consistency				
Type-1 (R)	1.0		1.0	
Type-2	0.39 (0.21–0.75)	0.004	0.46 (0.24–0.89)	0.022
Type-3	0.53 (0.18–1.58)	0.257	0.76 (0.23–2.55)	0.656
Tumor size				
Micro adenoma (R)	1.0		1.0	
Macro/giant adenoma	0.17 (0.05–0.57)	0.004	0.26 (0.08–0.91)	0.035
Cavernous sinus invasion				
Yes	0.16 (0.07–0.35)	<0.001	0.19 (0.08–0.44)	<0.001
No (R)	1.0		1.0	
Tumor consistency ^d				
Type-2				
E-kadherin staining				
No/weak (R)	1.0		1.0	
Strong	0.003 (0.001–0.010)	<0.001	0.005 (0.001–0.020)	<0.001
T2-MRI				
Hypo-intense (R)	1.0		1.0	
Iso-intense	9.67 (3.25–28.82)	<0.001	5.34 (0.99–28.56)	0.051
Hyper-intense	29.83 (13.32–66.77)	<0.001	7.86 (2.21–27.95)	0.001
Type-3				
E-kadherin staining				
No/weak (R)	1.0		1.0	
Strong	0.087 (0.027–0.281)	<0.001	0.09 (0.03–0.31)	<0.001
T2-MRI				
Hypo-intense (R)	1.0		1.0	
Iso-intense	5.64 (1.50–21.18)	0.010	4.28 (0.99–18.60)	0.052
Hyper-intense	1.69 (0.41–6.93)	0.464	0.81 (0.16–3.99)	0.795

Table 2. Univariable and multivariable logistic regression analyses. SG-A: Sparsely granulated adenoma, DG-A: Densely granulated adenoma, CS: Cavernous sinus, GTR: Gross total resection, STR: Subtotal resection. R: Reference category, OR: Odds ratio, aOR: Adjusted odds ratio, CI: Confidence interval. ^aReference category is “No”. ^bReference category is “DG-A”. ^cReference category is “STR”. ^dReference category is “Type-1”.

E-cadherin and β -catenin. No or weak staining for E-cadherin and β -catenin was observed in 8%, 97%, and 50% of the patients in the Type-1, Type-2, and Type-3 groups, respectively. The rate of no or weak staining for E-cadherin and β -catenin was very similar between Type-2 tumors and SG-A (97% vs. 95.5%). Furthermore, logistic regression analysis revealed that no or weak staining for E-cadherin was a predictor of Type-2 tumors ($p < 0.001$). Thus, the loss of E-cadherin and β -catenin results in the loss of cell–cell adhesion in tumors, as observed in Type-2 tumors. The loss of the ability of tumor cells to adhere to each other causes the tumor to exhibit a fluidic-mucinous form within itself and to exhibit a more invasive behavior to surrounding tissues. Although it may seem that fluidic-mucinous consistency can be easily resected, resection of these adenomas is more challenging compared to the Type-1 group due to their adhesive properties.

Tumor size, invasiveness, and consistency are reportedly associated with the success of surgical resection in pituitary adenomas. In patients with acromegaly, SG-A is more invasive and has a higher tumor volume than DG-A^{3,32–34}. These factors lead to the inadequate surgical resection and consequently lower remission rates in SG-As. However, the relationship between tumor consistency, which may affect surgical resection, and histopathological subtypes in patients with acromegaly has not been investigated. In our study, resection of Type-2 tumors were more challenging than the resection of Type-1 and Type-3 tumors due to its adhesive properties, invasive nature, and mucinous form. Thus, the likelihood of inadequate surgical resection increased in the Type-2 group. This was supported by the GTR rates in our study, with the GTR rate being significantly higher in the Type-1 than in the Type-2 group (79% vs. 60%; $p = 0.011$). However, it should not be overlooked that the relatively higher rate of patients with microadenoma in the Type-1 group compared to the Type-2 group (23% vs. 10%) may also contribute to the emergence of these resection rates. Furthermore, 89 patients with Type-1 tumor had DG-A and 95 patients with Type-2 had SG-A. Thus, the inadequate surgical resection and low remission rates in SG-As may be associated with the Type-2 tumor consistency in addition to tumor volume and invasiveness. Our study findings demonstrate that the surgical team should anticipate a more challenging resection when they encounter a Type-2 adenoma intraoperatively. Furthermore, considering the higher probability of an SG-A diagnosis, a more aggressive surgical strategy should be implemented to increase the likelihood of remission.

Despite studies demonstrating no statistical difference in the postoperative remission rate among the subtypes of somatotroph adenomas^{4,35,36}, it is widely accepted DG-A is associated with a higher remission rate than SG-A^{32,37–40}. In our study, the early postoperative remission rate of DG-As was significantly higher than that of SG-As (72.0% vs. 55.9%; $p = 0.017$). Furthermore, the early postoperative remission rate was significantly higher in the Type-1 group than in the Type-2 group (75% vs. 53%; $p = 0.004$). Moreover, multivariate analysis revealed that Type-1 tumors were a strong predictor of DG-A ($p < 0.001$). These findings support a potential relationship between Type-1 tumor consistency and a DG-A. Therefore, surgical teams who encounter Type-1 tumors intraoperatively can expect a remission success similar to that of DG-A and a good prognosis.

Preoperative MRI in patients with acromegaly can provide insights into the adenoma subtype, with a hyperintense appearance on T2-weighted sequences being highly associated with SG-A^{24,25,41,42}. In our study, 87.9% of the SG-As appeared hyperintense on the preoperative T2-weighted MR images. Significantly more SG-As were hyperintense than hypointense and isointense ($p < 0.001$ and $p = 0.001$, respectively). Among the 91 patients with a hyperintense lesion, 74 (81.3%) were Type-2 tumors. Univariate analysis hyperintense adenomas were more significantly associated with the Type-2 group than the Type-1 and Type-3 groups ($p < 0.001$ and $p < 0.001$, respectively). Furthermore, hypointense lesions were more significantly associated with the Type-1 group than with the Type-2 group ($p < 0.001$). Multivariate analysis revealed that hyperintense lesions were predictive of Type-2 tumors ($p = 0.001$). Thus, evaluation of preoperative T2-weighted MR images can help predict the histopathological subtype of somatotroph adenomas as well as the intraoperative tumor consistency. Preoperative knowledge of the tumor consistency could facilitate better planning of the surgical procedures and providing the patient with more detailed information.

If surgical remission cannot be achieved in somatotroph adenomas, priority is given to medical treatment, but radiosurgery is also planned if necessary. SG-As are more resistant to medical treatment than DG-As⁴³. This is because low SSTR-2 expression is associated with SG-As, whereas high cAMP levels are associated with DG-As^{43,44}. In our study, adjuvant treatment was administered to patients who did not meet the remission criteria at the 3rd postoperative month. The response rate to adjuvant treatment was significantly higher in the patients with Type-1 tumor than in the patients with Type-2 tumor (80.8% vs. 26.7%). This supports the hypothesis that patients with Type-1 tumors may have a better prognosis even after inadequate surgery ($p < 0.001$).

This study has some limitations. The patient population of the Type-3 group was very limited in a study that was initially planned for only two tumor consistencies (Type-1 and Type-2). Therefore, the data of the Type-3 group may mask the true results. Although there were similarities in the clinical, prognostic, and histopathological outcomes between the Type-1 tumors and DG-A, as well as between the Type-2 tumors and SG-A, the presence of other subtypes, which has been described as ‘intermediate form’, in somatotroph adenomas necessitates genetic studies to validate these results. Another limitation of the study is that the grading system for patients is inherently subjective and therefore closely related to the surgeon’s experience.

Conclusions

The current suboptimal rates of surgical remission in patients with acromegaly have led to the exploration of different surgical strategies. This study demonstrates that surgeon could predict the prognosis and histopathological subtype of the somatotroph adenoma by observing the tumor consistency intraoperatively. This could facilitate better planning of patient-specific surgical strategies during the operation to increase the remission rate. However, further genetic studies aimed at studying the unclear ‘intermediate form’ in detail and evaluating the relationship between tumor consistencies and newly emerging subtypes are required. This will further improve the planning of personalized surgical treatments.

Data availability

The data and materials of the patients used in the study are in the archive of our hospital. The datasets used and/or analysed during the current study available from the corresponding author on reasonable request.

Received: 3 August 2024; Accepted: 1 January 2025

Published online: 06 January 2025

References

- Asa, S. L. *Tumors of the Pituitary Gland* (American Registry of Pathology, 1998).
- Horvath, E. & Kovacs, K. The adenohypophysis. In *Functional Endocrine Pathology* (eds Kovacs, K. & Asa, S. L.). vol. 1, 245–281 (Blackwell, 1991).
- Asa, S. L., Mete, O., Perry, A. & Osamura, R. Y. Overview of the 2022 WHO classification of pituitary tumors. *Endocr. Pathol.* **33**(1), 6–26 (2022).
- Akirov, A., Asa, S. L., Amer, L., Shimon, I. & Ezzat, S. The clinicopathological spectrum of acromegaly. *J. Clin. Med.* **8**(11), 1962 (2019).
- Melmed, S., Braunstein, G. D., Horvath, E. V. A., Ezrin, C. & Kovacs, K. Pathophysiology of acromegaly. *Endocr. Rev.* **4**(3), 271–290 (1983).
- Sano, T., Ohshima, T. & Yamada, S. Expression of glycoprotein hormones and intracytoplasmic distribution of cytokeratin in growth hormone-producing pituitary adenomas. *Pathology-Research Pract.* **187**(5), 530–533 (1991).
- Yamada, S. et al. Growth hormone-producing pituitary adenomas: correlations between clinical characteristics and morphology. *Neurosurgery* **33**(1), 20–27 (1993).
- Obari, A. et al. Clinicopathological features of growth hormone-producing pituitary adenomas: difference among various types defined by cytokeratin distribution pattern including a transitional form. *Endocr. Pathol.* **19**, 82–91 (2008).
- Swanson, A. A. et al. Clinical, biological, radiological, and pathological comparison of sparsely and densely granulated somatotroph adenomas: a single center experience from a cohort of 131 patients with acromegaly. *Pituitary*. **24**, 192–206 (2021).
- Kato, M. et al. Differential expression of genes related to drug responsiveness between sparsely and densely granulated somatotroph adenomas. *Endocrine journal*. **59**(3), 221–228 (2012).
- Mayr, B. et al. Molecular and functional properties of densely and sparsely granulated GH-producing pituitary adenomas. *Eur. J. Endocrinol.* **169**(4), 391–400 (2013).
- Anik, I. et al. Endoscopic transsphenoidal approach for acromegaly with remission rates in 401 patients: 2010 consensus criteria. *World Neurosurg.* **108**, 278–290 (2017).
- Heck, A., Emblem, K. E., Casar-Borota, O., Bollerslev, J. & Ringstad, G. Quantitative analyses of T2-weighted MRI as a potential marker for response to somatostatin analogs in newly diagnosed acromegaly. *Endocrine* **52**, 333–343 (2016).
- Babu et al. Long-term endocrine outcomes following endoscopic endonasal transsphenoidal surgery for acromegaly and associated prognostic factors. *Neurosurgery*. **81**(2), 357–366 (2017).
- Nishioka, H., FukuHara, N., Horiguchi, K. & Yamada, S. Aggressive transsphenoidal resection of tumors invading the cavernous sinus in patients with acromegaly: predictive factors, strategies, and outcomes. *J. Neurosurg.* **121**(3), 505–510 (2014).
- Briceno, V. et al. Efficacy of transsphenoidal surgery in achieving biochemical cure of growth hormone-secreting pituitary adenomas among patients with cavernous sinus invasion: a systematic review and meta-analysis. *Neurol. Res.* **39**(5), 387–398 (2017).
- Campbell, P. G. et al. Outcomes after a purely endoscopic transsphenoidal resection of growth hormone-secreting pituitary adenomas. *NeuroSurg. Focus*. **29**(4), E5 (2010).
- Shirvani, M. & Motiei-Langroudi, R. Transsphenoidal surgery for growth hormone-secreting pituitary adenomas in 130 patients. *World Neurosurg.* **81**(1), 125–130 (2014).
- Yilmaz, M., Vural, E., Kenan, K. O. C. & Ceylan, S. Cavernous sinus invasion and effect of immunohistochemical features on remission in growth hormone secreting pituitary adenomas. *Turkish Neurosurg.* **25**(3) (2015).
- Rutkowski, M. J. et al. Development and clinical validation of a grading system for pituitary adenoma consistency. *J. Neurosurg.* **134**(6), 1800–1807 (2020).
- Acitores Cancela, A. et al. Clinical relevance of tumor consistency in pituitary adenoma. *Hormones* **20**(3), 463–473 (2021).
- Acitores Cancela, A., Berrocal, R., Pian Arias, V., Díez, H., Iglesias, P. & J. J., & Effect of pituitary adenoma consistency on surgical outcomes in patients undergoing endonasal endoscopic transsphenoidal surgery. *Endocrine* **78**(3), 559–569 (2022).
- Giustina, A. et al. Multidisciplinary management of acromegaly: a consensus. *Rev. Endocr. Metab. Disord.* **21**(4), 667–678. <https://doi.org/10.1007/s11154-020-09588-z> (2020). Epub 2020 Sep 10.
- Heck, A. et al. Intensity of pituitary adenoma on T2-weighted magnetic resonance imaging predicts the response to octreotide treatment in newly diagnosed acromegaly. *Clin. Endocrinol.* **77**(1), 72–78 (2012).
- Tang, Y. et al. Analysis of diffusion-weighted and T2-weighted imaging in the prediction of distinct granulation patterns of somatotroph adenomas. *World Neurosurg.* **182**, e334–e343 (2024).
- Mete, O. K. M., Osamura, R. Y., Trouillas, J. & Yamada, S. Somatotroph adenoma. In *WHO Classification of Tumours of Endocrine Organs*, 4th edn. (eds Lloyd, R. V. O. R. et al.) 13–23 (International Agency for Research on Cancer (IARC), 2017).
- Xu, B., Sano, T., Yoshimoto, K. & Yamada, S. Downregulation of E-cadherin and its undercoat proteins in pituitary growth hormone cell adenomas with prominent fibrous bodies. *Endocr. Pathol.* **13**, 341–351 (2002).
- Takeichi, M. Cadherin cell adhesion receptors as a morphogenetic regulator. *Science* **251**(5000), 1451–1455 (1991).
- Gumbiner, B. M. Cell adhesion: the molecular basis of tissue architecture and morphogenesis. *Cell* **84**(3), 345–357 (1996).
- Auerkari, E. I. Methylation of tumor suppressor genes p16 (INK4a), p27 (Kip1) and E-cadherin in carcinogenesis. *Oral Oncol.* **42**(1), 4–12 (2006).
- Sano, T., Rong, Q. Z., Kagawa, N. & Yamada, S. Down-regulation of E-cadherin and catenins in human pituitary growth hormone-producing adenomas. *Front. Horm. Res.* **32**, 127–132 (2004).
- Kiseljak-Vassiliades, K. et al. Growth hormone tumor histological subtypes predict response to surgical and medical therapy. *Endocrine* **49**, 231–241 (2015).
- Heng, L. et al. Preoperative prediction of granulation pattern subtypes in GH-secreting pituitary adenomas. *Clin. Endocrinol.* **95**(1), 134–142 (2021).
- Cuevas-Ramos, D. et al. A structural and functional acromegaly classification. *J. Clin. Endocrinol. Metabolism.* **100**(1), 122–131 (2015).
- Brzana, J., Yedinak, C. G., Gultekin, S. H., Delashaw, J. B. & Fleseriu, M. Growth hormone granulation pattern and somatostatin receptor subtype 2A correlate with postoperative somatostatin receptor ligand response in acromegaly: a large single center experience. *Pituitary* **16**, 490–498 (2013).
- Akkus, G. et al. Novel classification of acromegaly in accordance with immunohistochemical subtypes: is there really a clinical relevance? *Horm. Metab. Res.* **54**(01), 37–41 (2022).
- Vuong, H. G. & Dunn, I. F. Clinical and prognostic significance of granulation patterns in somatotroph adenomas/tumors of the pituitary: a meta-analysis. *Pituitary* **26**(6), 653–659 (2023).

38. Wang, L. et al. Clinicopathological analysis of densely and sparsely granulated somatotroph tumors of pituitary. *World Neurosurgery*. (2024).
39. Yan, J. L. et al. Surgical outcome and evaluation of strategies in the management of growth hormone-secreting pituitary adenomas after initial transsphenoidal pituitary adenectomy failure. *Front. Endocrinol.* **13**, 756855 (2022).
40. Mazal, P. R. et al. Prognostic relevance of intracytoplasmic cytokeratin pattern, hormone expression profile, and cell proliferation in pituitary adenomas of akromegalic patients. *Clin. Neuropathol.* **20**(4), 163–171 (2001).
41. Park, Y. W. et al. Radiomics model predicts granulation pattern in growth hormone-secreting pituitary adenomas. *Pituitary* **23**, 691–700 (2020).
42. Hagiwara, A. et al. Comparison of growth hormone-producing and non-growth hormone-producing pituitary adenomas: imaging characteristics and pathologic correlation. *Radiology* **228**(2), 533–538 (2003).
43. Ezzat, S. et al. Predictive markers for postsurgical medical management of acromegaly: a systematic review and consensus treatment guideline. *Endocrine Practice*, **25**(4), 379–393 (2019).
44. Asa, S. L. & Ezzat, S. An update on pituitary neuroendocrine tumors leading to acromegaly and gigantism. *J. Clin. Med.* **10**(11), 2254 (2021).

Author contributions

E.Y. Writing—original draft, software, visualization. S.D.O. Histopathological examination. A.U. Software, resources, investigation. P.Y. Software, resources, investigation. A.E. resources, investigation. A.G. formal analysis, data curation. M.Ç. formal analysis, data curation. S.B. Statistical analysis evaluation. A.E.D. Histopathological examination. B.Ç. Supervision, writing—review and editing. I.A. Supervision, writing—review and editing. S.C. Conceptualizations, methodology, project administration.

Declarations

Competing interests

The authors declare no competing interests.

Additional information

Supplementary Information The online version contains supplementary material available at <https://doi.org/10.1038/s41598-025-85331-5>.

Correspondence and requests for materials should be addressed to S.C.

Reprints and permissions information is available at www.nature.com/reprints.

Publisher's note Springer Nature remains neutral with regard to jurisdictional claims in published maps and institutional affiliations.

Open Access This article is licensed under a Creative Commons Attribution-NonCommercial-NoDerivatives 4.0 International License, which permits any non-commercial use, sharing, distribution and reproduction in any medium or format, as long as you give appropriate credit to the original author(s) and the source, provide a link to the Creative Commons licence, and indicate if you modified the licensed material. You do not have permission under this licence to share adapted material derived from this article or parts of it. The images or other third party material in this article are included in the article's Creative Commons licence, unless indicated otherwise in a credit line to the material. If material is not included in the article's Creative Commons licence and your intended use is not permitted by statutory regulation or exceeds the permitted use, you will need to obtain permission directly from the copyright holder. To view a copy of this licence, visit <http://creativecommons.org/licenses/by-nc-nd/4.0/>.

© The Author(s) 2025